

THE EFFECT OF SCANDIUM ON THE SOLIDIFICATION BEHAVIOUR OF ALUMINIUM ALLOYS

Andrew F. NORMAN and Philip B. PRANGNELL

Manchester Materials Science Centre, University of Manchester / UMIST,
Grosvenor Street, Manchester, M1 7HS, U.K.

ABSTRACT The solidification behaviour of binary Al-Sc alloys have been investigated for both hypo- and hyper-eutectic alloy compositions. Sc additions greater than 0.55 wt.% (the eutectic point) produce a substantial refinement in the grain size of aluminium castings, which is due to the formation of the primary Al_3Sc intermetallic phase during solidification. The refinement in grain size occurs because the $L1_2 Al_3Sc$ phase is almost identical to the crystal structure and lattice parameter of Al, which nucleates epitaxially on its surface. The grain refinement is accompanied by a change in the growth morphology from dendritic in the large un-refined castings, to fine spherical grains in the refined castings. On cooling to room temperature, the Al-Sc supersaturated solid solution decomposes via a discontinuous precipitation reaction to form coherent rod-like precipitates of the $L1_2 Al_3Sc$ phase.

Keywords: Al-Sc Alloys, Solidification, Grain Refinement, Microstructure, TEM.

1. INTRODUCTION

In the former Soviet Union, there have been a number of Al alloys developed in the last 20 years which contain additions of Sc [1]. The main published claims for the benefits of adding Sc include: a substantial age hardening response [2], inhibition of recrystallisation [3], grain refinement of cast ingots [4,5], and improvements in weldability [6]. These effects have often been linked to some of the unique features of the Al-Sc equilibrium phase diagram which is dominated at the Al-rich end by a eutectic reaction between α -Al and the Al_3Sc intermetallic phase (Fig. 1a). The phase diagram is unusual in that the eutectic temperature occurs only slightly below the melting point of Al, and at the low Sc level of 0.55 wt.%. The equilibrium Al_3Sc compound which forms at the Al-rich end of the phase diagram has an ordered $L1_2$ crystal structure with a lattice parameter close to that of Al [7]. In contrast to this, the most commonly used transition metal grain refining additions (Ti and Zr) form peritectic reactions with Al and only form the $L1_2 Al_3X$ ($X=Ti$ or Zr) compound as a metastable phase [8].

Despite the claimed grain refining ability of Sc, most of the published data has concentrated on the decomposition of the Al-Sc supersaturated solid solution, and there is little available detailed information concerning the solidification behaviour of Al-Sc alloys. Therefore, the main focus of this paper is to explore the solidification behaviour of Al-Sc alloys and the important issue of scandium's ability to strongly refine cast ingots. Two compositions were chosen for study; a dilute Al - 0.2 wt.% Sc hypoeutectic alloy, and the more concentrated hypereutectic composition of Al - 0.7 wt.% Sc. The as-cast microstructures were characterised using a combination of optical metallography, SEM and TEM. The role of the $L1_2 Al_3Sc$ primary intermetallic particles as efficient nucleation sites for the α -Al matrix was explored.

2. EXPERIMENTAL

The cast samples were prepared from commercial purity Al and an Al-2 wt.% Sc master alloy, and cast into a wedge shaped copper mould. The mould was designed to give cooling rates in the range $100 K s^{-1}$ (top surface) to $1000 K s^{-1}$ (wedge tip). To reveal the grain structures, the samples were anodised using Barker's reagent and viewed under polarised light. For SEM

examination, samples were lightly electropolished in a solution of 5 vol.% Perchloric Acid in methanol at -30°C and 20 V. These samples were subsequently carbon coated and examined in a Philips 525 SEM, operated at 20 kV. Electron back scattered diffraction (EBSD) analysis of the constituent phases was carried out in a JEOL 6300 SEM. Thin foils for TEM examination were prepared by grinding sections of the wedge casting to thin sheet and punching out 3 mm diameter discs, which were then electropolished in a solution of 30 vol.% Nitric Acid in Methanol at -30°C and 16 V. The foils were examined in a Philips CM200 TEM operated at 200 kV. The mean linear intercept method was used to measure the average grain size in the castings [9].

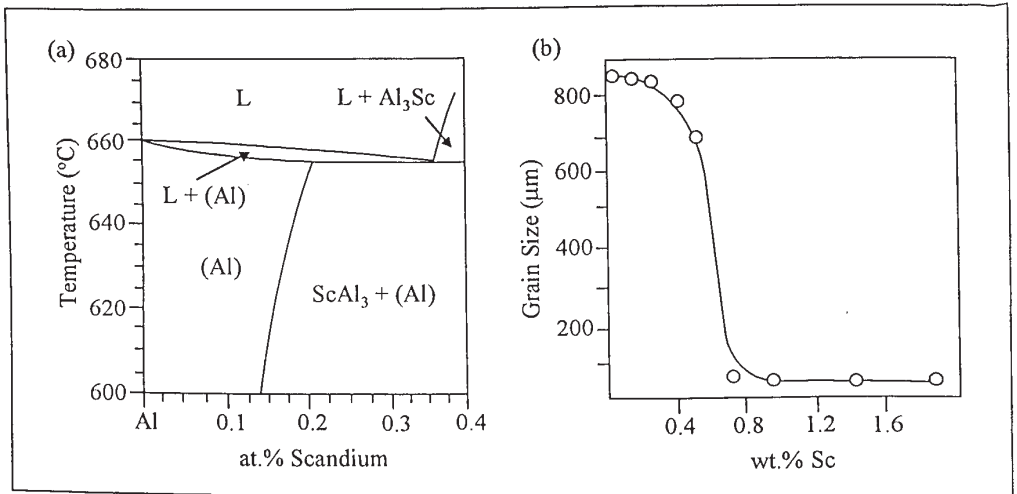


Figure 1: (a) Al-rich end of the Al-Sc equilibrium phase diagram [7], (b) Plot of grain size vs Sc addition to high purity Al [5].

3. RESULTS AND DISCUSSION

3.1 Solidification Behaviour of binary Al-Sc Castings

Typical microstructures for the two Al-Sc compositions are shown in Fig. 2 for the applied cooling rate of 100 K s^{-1} . Also shown in Fig. 2 is the microstructure obtained for an Al-4.5 wt.% Cu alloy which contained no grain refining additions. With the hypoeutectic alloy (0.2 wt.% Sc), a large grain size was observed throughout the casting which was comparable to that seen in the Al-Cu casting, demonstrating that there is no grain refinement apart from that due to solute effects. In sharp contrast, an exceptionally fine grain size was observed in the hypereutectic alloy (0.7 wt.% Sc) which is two orders of magnitude finer ($\sim 80\ \mu\text{m}$ compared to $\sim 1\ \text{mm}$). These results are in good agreement with the work of Lamikov and Samsonov [4] and Drits *et al.* [5] whose data is replotted in Fig. 1b. The reasons for this exceptional grain refinement will be discussed in section 3.2.

The sub-structures of the two Al-Sc castings were also examined in more detail. In the unrefined casting (0.2 wt.% Sc), a dendritic sub-structure could be seen, which is often associated with the solidification behaviour of hypoeutectic alloys. For this composition, the first phase to solidify is clearly α -Al which nucleates on the mould wall as large columnar grains. In the hypereutectic alloy (0.7 wt.% Sc) there is a total absence of columnar grains and a lack of dendritic sub-structure within the fine grains. Here, the first phase to solidify, on crossing the liquidus, is the $\text{L}_{12}\text{Al}_3\text{Sc}$ phase which precipitates as primary intermetallic particles in the liquid. Under equilibrium

conditions, the remaining liquid should solidify isothermally at the eutectic temperature, by the coupled growth of the α -Al and Al_3Sc phases. Fig. 3 shows a primary faceted Al_3Sc particle on which the α -Al grain has nucleated and grows outwards. In this figure there is no evidence for coupled growth. This behaviour is typical of that observed for a "divorced" eutectic and is consistent with the difficulty of coupled growth, when the volume fractions of one phase is very small, due to the dilute nature of the eutectic composition, and when the growth kinetics of the Al_3Sc phase is slow relative to that of α -Al (this assumption is reasonable given the faceted nature of the primary particles). The formation of a divorced eutectic would also require the very efficient nucleation of the α -Al phase on the primary Al_3Sc particles, which is consistent with the remarkable grain refining effect seen in Fig. 2. It is worth noting that there could still be no dendritic sub-structure within the grains even if the α -Al phase tried to grow dendritically, if the grain size is refined to such an extent that the grain diameter is the same order of magnitude as the dendrite tip radius at the cooling rates used.

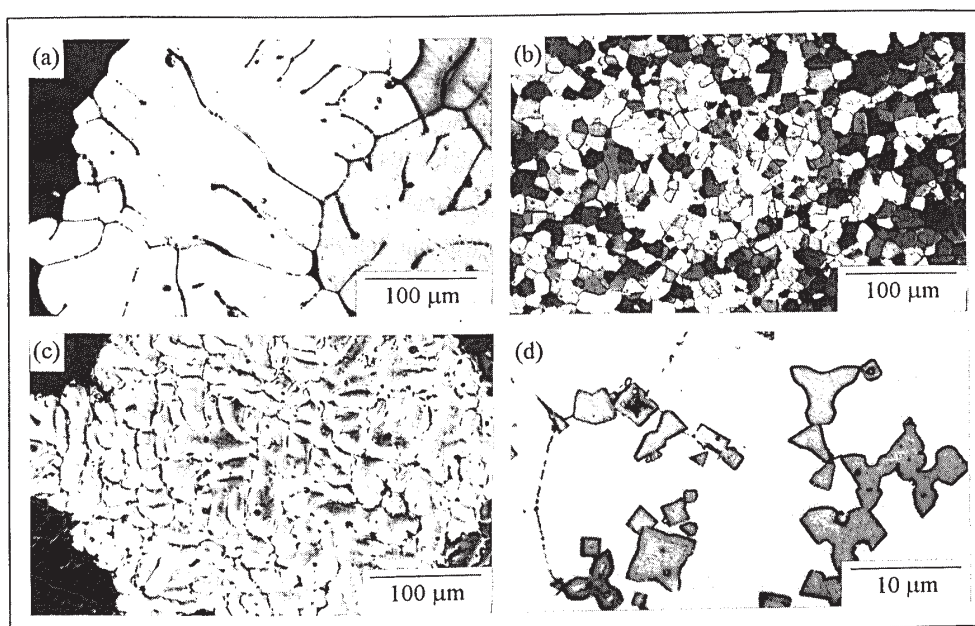


Figure 2: Examples of the solidification microstructures, (a) 0.2 wt.% Sc, (b) 0.7 wt.% Sc, (c) 4.5 wt.% Cu. (d) Example of the $L1_2$ Al_3Sc morphology in the Al-2 wt.% Sc master alloy.

3.2 Morphology and Grain Refining Ability of the $L1_2$ Al_3Sc Primary Intermetallic

In order to be able explain the exceptional grain refining effect of Sc on aluminium, which occurs only in hypereutectic alloys, it is necessary to examine the morphology of the primary Al_3Sc particles and their role as potential heterogeneous nucleation sites for the α -Al phase.

(i) Morphology of the Primary $L1_2$ Al_3Sc Intermetallic Particles

Examples of the primary $L1_2$ Al_3Sc intermetallic particles that form in the hypereutectic Al-Sc alloys are shown in Fig. 2d. From Fig. 2d it is immediately apparent that they are highly faceted, but appear as range of shapes in two-dimensional sections, based on squares, stars and triangles. Similar shaped particles have been observed in rapidly solidified Al-Zr [8] and Al-Hf [10] alloys, and were identified as being primary $L1_2$ Al_3Zr and $L1_2$ Al_3Hf particles with a cusped cubic

morphology, which were sectioned along different crystallographic directions [8]. It is thus apparent that the $L1_2$ Al_3Sc particles have a similar morphology.

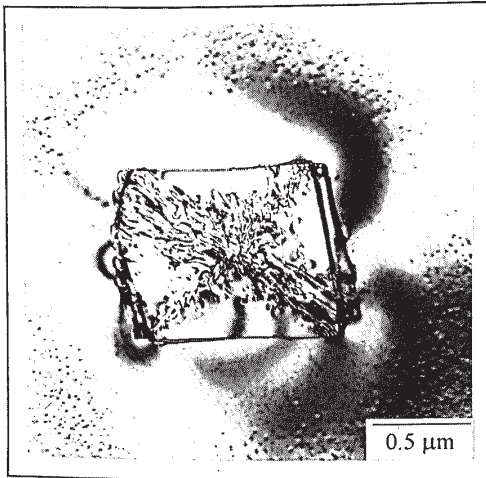


Figure 3: TEM micrograph showing a primary $L1_2$ Al_3Sc intermetallic particle.

The primary $L1_2$ Al_3Sc particles were also examined in the TEM. The $L1_2$ crystallographic structure was confirmed using selected area diffraction patterns which revealed the presence of superlattice reflections. The lattice parameter of the Al_3Sc intermetallic was determined as 0.4104 nm from X-ray diffraction measurements made on the hypereutectic alloy which is in good agreement with the measurements of Blake and Hopkins [11]. Fig. 3 shows that as well as being clearly faceted, the primary particles also exhibit internal strain contrast, that can be interpreted as being caused by local compositional fluctuations. The internal "structure" can be seen to appear as dendritic and originate from the centre of the particle and grows towards the corners of the cube. Similar internal structures have also been observed in chill cast Al-Hf [10] and Al-Zr [8] alloys and were attributed to the dendritic nature of the

growth of the particles in the liquid. This suggests that the depiction of the Al_3Sc phase on the phase diagram as a simple line compound in Ref. [7] is incorrect, and that it actually exists over a limited range of compositions.

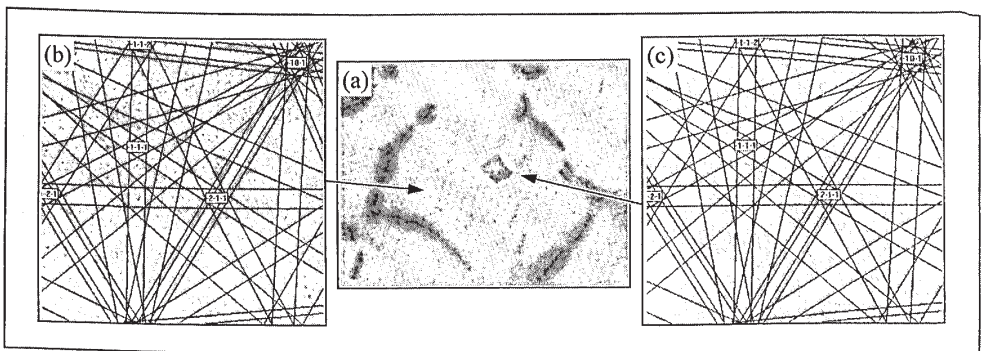


Figure 4: EBSD pattern analysis for the Al - 0.7 wt.% Sc alloy. (a) SEM micrograph showing the $L1_2$ Al_3Sc particle, (b) Kikuchi pattern for the α -Al matrix, and (c) Kikuchi pattern for the particle.

(ii) *The Grain Refining Efficiency of the Primary $L1_2$ Al_3Sc Intermetallic Particles*

The microstructures in Fig. 2, and the results described above, demonstrate the exceptional nucleation efficiency of α -Al in the hypereutectic alloy, caused by the presence of the $L1_2$ Al_3Sc intermetallic particle. Because of the similarities between the crystal structures of the two α -Al and Al_3Sc phases, the heterogeneous nucleation of α -Al would be expected to lead to the epitaxial growth of α -Al on the $L1_2$ Al_3Sc particles. To investigate this possibility, the technique of electron

back scattered diffraction (EBSD) was used in the SEM to measure the misorientation difference between several $L1_2$ Al_3Sc particles and the surrounding Al-grains.

An example of a grain containing an $L1_2$ Al_3Sc particle, together with the associated EBSD patterns obtained from each phase, are shown in Fig. 4. In Fig. 4, the grain contains an Al_3Sc particle in its centre and the misorientation between the particle and matrix was calculated from the diffraction patterns to be less than 1° (which is of the order of the accuracy of the measurement) indicating that the α -Al matrix has, as anticipated, nucleated and grown epitaxially on the Al_3Sc particle. In contrast to this observation, some grains contained Al_3Sc particles that were not epitaxially related to the Al matrix. This might be expected as, although the $L1_2$ Al_3Sc particle is a very efficient nucleant for the α -Al matrix, not all of the particles will act as nucleants for the matrix phase. Those particles which do not act as nucleants will be pushed to the grain boundaries by the advancing solid/liquid interface during solidification.

3.3 Decomposition of the Supersaturated Al-Sc Solid Solution

In the Al - 0.7 wt.% Sc alloy, TEM revealed that the centre of many of the grains contained a fine scale precipitation of small homogeneously nucleated coherent spherical particles. These were identified as also being the $L1_2$ Al_3Sc phase. Fig.3 shows a primary faceted Al_3Sc particle, which formed during the first stage of solidification, surrounded by very fine spherical Al_3Sc particles nucleated from solid solution on cooling. Also evident in Fig. 3 is a precipitate free zone, which surrounds the primary $L1_2$ Al_3Sc cubic particle. This suggests that the primary cubic particle continued to grow in the solid state during cooling to room temperature, consuming some solute from the surrounding region.

During further TEM examination of the Al - 0.7 wt.% Sc as cast samples, some of the grains appeared irregular in shape. On closer examination, it was apparent that these grain boundaries had migrated on cooling, via a discontinuous precipitation reaction, leaving a fan shaped array of precipitates behind the moving grain boundary. The aspect ratio of these precipitates varied between 10 and 50 with a separation of 0.1 to 0.2 μm . Selected area diffraction of these precipitates confirmed the presence of superlattice reflections, which is indicative of the coherent $L1_2$ Al_3Sc phase, and they are imaged in dark field in Fig. 5. Similar discontinuous precipitation reactions have been widely reported in Al alloys containing $L1_2$ Al_3X phases; including δ' in Al-Li [10], and β' in Al-Zr [13] and Al-Hf [10] alloys. The widely accepted mechanism for this type of discontinuous precipitation reaction is that the supersaturated solid solution decomposes behind a grain boundary, which is pushed forwards by the developing precipitates [12-14]. However in the Al-Li, Al-Zr and Al-Hf alloy systems, the discontinuous precipitates are metastable and the transformation is inhibited by the formation of the equilibrium phases at grain boundaries [12]. This cannot occur in the Al-Sc system because the precipitates that form in the solid state are already an equilibrium phase. However, the grain boundaries can be pinned locally by the presence of eutectic particles which form prior to the discontinuous precipitates.

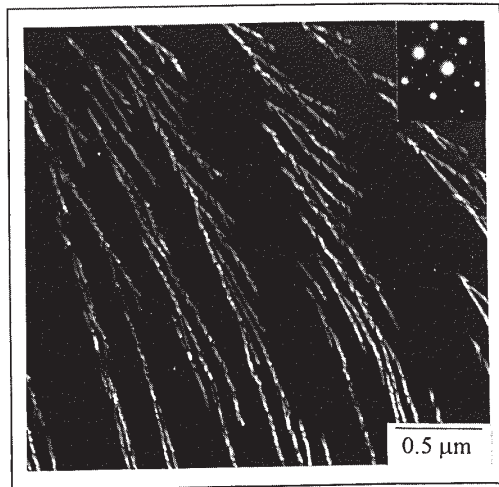


Figure 5: TEM micrograph showing the rod-like morphology of the $L1_2$ Al_3Sc discontinuous precipitates.

4. CONCLUSIONS

1. Effective grain refinement can be achieved in binary Al-Sc alloys for compositions greater than 0.55 wt.% (the eutectic composition). This is attributed to the formation of the L_{12} Al_3Sc phase as primary particles in the liquid, which act as efficient nucleation sites for the α -Al phase.
2. The grain refinement is accompanied by a change in the growth morphology from large dendritic grains, in the un-refined casting, to fine spherical grains in the refined casting. The lack of a sub-structure within the fine spherical grains is attributed to formation of a "divorced" eutectic.
3. On cooling to room temperature, the Al-Sc supersaturated solid solution decomposes via a discontinuous precipitation reaction to form coherent rod-like precipitates of the L_{12} Al_3Sc phase.

5. ACKNOWLEDGEMENTS

This work was supported by the EPSRC under the IMI Programme, Grant: GR/K66901, and is released with the kind permission of the following partners: British Aerospace, Short Brothers, DERA, Rolls Royce, British Aluminium, TWI, University of Liverpool, Cranfield University and the University of Essex. The authors thank Dr R. Elliott and Dr V.V. Zakharov for some very helpful discussions.

6. REFERENCES

- [1] I.N. Frindlyander, A.G. Bratukhin and V.G. Davidov: Proc. 6th Int. Conf. On Al-Li Alloys, (edited by M. Peters and P.J. Winkler), Garmisch-Partenkirchen, DGM Informationsgesellschaft, Oberursel, Germany, p. 35 (1992).
- [2] M.E. Drits, L.B. Ber, Y.G. Bykov and L.S. Toropova: Physics of Metals and Physical Metallurgy (USSR), 57 (1984), 1172.
- [3] M.E. Drits, L.S. Toropova, Y.G. Bykov, L.B. Ber and S.G. Pavlenko: Russian Metallurgy (USSR), No. 1 (1982), 148.
- [4] L.K. Lamikov and G.V. Samsonov: Soviet Non-Ferrous Metals Research (USSR), No. 8 (1964), 79.
- [5] M.E. Drits, L.S. Toropova, Y.G. Bykov, F.L. Guschina, V.I. Yelagin and Y.A. Filatov: Russ. Met. (USSR), No. 1 (1983), 150.
- [6] B. Irving: Welding Journal, 76 (1997), 53.
- [7] K.A. Gschneidner and F.W. Calderwood: Bull. Alloy Phase Diag., 10 (1989), 34.
- [8] S. Hori, S. Saji and A. Takehara: Proc. 4th Int. Conf. On Rapidly Quenched Metals, (edited by T. Masumoto and K. Suzuki), Japan Institute of Metals, p. 1545 (1982).
- [9] F.B. Pickering: Basis of Quantitative Metallography, Institute of Metals (1975).
- [10] A.F. Norman and P. Tsakirooulos: Int. J. Rapid Solid., 6 (1991), 185.
- [11] N. Blake and M.A. Hopkins: J. Materials Science, 20 (1985), 185.
- [12] P.B. Prangnell, D. Özkaya and W.M. Stobbs: Acta Metall., 42 (1994), 419.
- [13] E. Nes and H. Billdal: Acta Metall., 25 (1977), 1039.
- [14] D.B. Williams and E.P. Butler: Internat. Mater. Rev., No.3 (1981), 153.